A new type of fiber-optic-based interferometric ellipsometer for in situ and real-time measurements

Suat Topsu, Luc Chassagne, Yasser Alayli

A new type of fiber-optic-based interferometric ellipsometer for *in situ* and real-time measurements

S. Topcu,[a] L. Chassagne, and Y. Alayli
Laboratoire LIRIS, Université de Versailles, 45 Avenue des états-unis, 78035 Versailles, France

(Received 20 March 2003; accepted 23 June 2003)

It is shown that it is possible to improve interferometric ellipsometers by using a Pockels cell or a Bragg cell hence avoiding the use of any moving components. Furthermore, these methods allow one to increase the beat frequency signal permitting a better insensitiveness to mechanical disturbances. It is also shown how to incorporate an optical fiber between the neutral beam splitter and the sample without losing any information concerning the ellipsometric angles of the sample. Several configurations are described and theoretically analyzed. The last ones do not contain any active component around the sample. They offer a new measurement technique for real-time and *in situ* measurements. © *2003 American Institute of Physics.* [DOI: 10.1063/1.1606118]

I. INTRODUCTION

Ellipsometry is a powerful tool for optical characterization of surfaces and thin films. Ellipsometric techniques use the fact that the reflection of linearly or circularly polarized light from a material is accompanied by a change in the phase and intensity of the composite components giving, in general, elliptically polarized light. The change in polarization depends on the surface properties. It allows the optical properties such as refractive index, absorption index, optical thickness, and birefringence of optical surfaces or thin films to be determined. Electromagnetic waves are characterized by an electric field vector **E** oscillating in a direction perpendicular to a magnetic field vector **B**. Here, we refer only to the electric field. Its direction can be expressed in terms of two independent and perpendicular directions, which are referred to as *s* and *p* directions. These two directions lie in a plane perpendicular to the propagation one. The direction *p* is at 90° with respect to the direction of propagation, while direction *s* points out of the plane of the page.

The measured ellipsometric parameters are defined through the fundamental formula:

$$\rho = \frac{r_p}{r_s} = \tan(\psi) \times \exp(j\Delta), \tag{1}$$

where r_p and r_s represent, respectively, the reflectivity coefficient for the *p* and *s* direction of polarization. $\tan(\psi)$ and Δ are, respectively, amplitude ratio and phase difference of the *p* and *s* components of the reflected light. These angles are usually called the ''ellipsometric angles'' of the sample.

We propose various configurations for the realization of an ellipsometer which measurement is deported by means of optical fibers making them well suited for *in situ* measurements. All the proposed systems are based on the principle of interferometric ellipsometers. The last configurations do not contain any active element (optical modulator, shutter) between the end of the optical fiber, the sample, and the measurement board.

II. PRINCIPLE OF AN INTERFEROMETRIC ELLIPSOMETER

A. The Hazebroek and Holscher ellipsometer

The interferometric ellipsometer was first developed in 1973 by Hazebroek and Holscher in the Shell Research Laboratory of Amsterdam.[1] It consists in using a frequency stabilized laser with a Michelson interferometer. The light source, a He–Ne laser, emits a beam of monochromatic unpolarized light of wavelength 632.9 nm. After passing the Glan–Thomson prism the light is linearly polarized, with the electric field set at 45° with respect to the normal plane of the measurement setup. Half the light of the beam is transmited (the reference beam) by a neutral density beam splitter and half is reflected (the measuring beam). With an adjustable angle of incidence, the measuring beam is then incident on a sample. The reflected beam is accurately autocollimated by a mirror, thus the beam is reflected a second time by the sample. The reference beam retraces its path after being reflected by a mirror moving at constant speed (attached to an electromagnetic driver). As a result the reference beam is Doppler-shifted. Both beams recombine at the back of the beam splitter. Interference occurs. The recombined beam is split into the two orthogonal polarization modes by the Wollaston prism. The intensities of the two polarizations are converted into ac voltages with frequencies equal to the Doppler shift. These electrical signals are then amplified and processed in the electronic part of the system. Finally, the ellipsometric angles of the sample can be deduced from the amplitude ratio and phase difference of the two electrical signals. A rigorous theoretical calculation can be found in Refs. 2 and 3.

The problem of the slowness of the Hazebroek and Holscher setup (8 s per measurement) is essentially due to the mechanical part of the system. The electromagnetic driver causes periodic motion of a mirror at approximately

[a]Electronic mail: suat.topcu@ens-phys.uvsq.fr

uniform speed. With $v=55\ \mu\mathrm{m\,s}^{-1}$ and $\lambda=632.9$ nm, one obtains a signal angular frequency of 175 Hz. Considerable averaging of the signals is required to remove fluctuations due to mechanical perturbations which are usually around some tens of hertz. Hence this method is only well-suited for measuring the optical properties of equilibrium systems or slow surface processes, such as corrosion or electrochemical film growth. In addition, such an interferometric ellipsometer has the advantage of not requiring a compensator, hence wideband operation is possible.

B. Notation

A relatively simple mathematical description of this type of ellipsometer is possible using Jones matrices calculation.[2] Here we consider only ideal optical components. Physical effects that have the same influence on both polarizations, such as absorption, can in fact be taken into account by means of reference measurements. In calculations, $N_{r,t}$, B, G, $W_{r,t}$, and M_0 refer to Jones matrices of, respectively, a 50/50 neutral density beam splitter, a polarizing beam splitter, a Glan–Thomson polarizer with its principal axis along the s direction, a Wollaston prism, and a mirror at normal incidence. The sample is a reflective-type optical device, represented by

$$S=\begin{pmatrix} r_s & 0 \\ 0 & r_p \end{pmatrix}, \tag{2}$$

where $r_s=|r_s|\exp(i\phi_s)$ and $r_p=|r_p|\exp(i\phi_p)$ are, respectively, the reflectivity coefficients for the s and p direction of polarization. Let φ be the angle over which the orientation of the element has been rotated with respect to s and p directions and X an arbitrary optical element, then it will be designed by $X(\varphi)$. As the final calculated parameter is the intensity of the wave, we have omitted all the phase factors in front of the Jones matrices.

III. IMPROVEMENT OF THE HAZEBROEK AND HOLSCHER ELLIPSOMETER

One solution to solve the problem of the slowness of the Hazebroek and Holscher ellipsometer would consist of increasing the frequency difference between the two beams. This solution has been proposed first by Umeda and Takasaki.[4] It is the combination of the Hazebroek and Holscher interfering ellipsometer with a two-frequency laser. A theoretical study of configurations using the Zeeman laser has been proposed by Wind and Hemmes.[3] Here, we propose other methods for increasing the frequency difference between the two beams based on the use of a low cost laser diode and a Pockels cell or a Bragg cell.

A. Configuration using a Bragg cell

1. Jones matrix of a Bragg cell

In the primary Hazebroek and Holscher ellipsometer, the Doppler shift is induced by a reflection of the light beam from a mirror that moves with a velocity v. The same behavior could be observed by a light beam passing through a Bragg cell. The incident light is reflected from surfaces that move with a velocity v_s. A Bragg cell is made of a flint glass

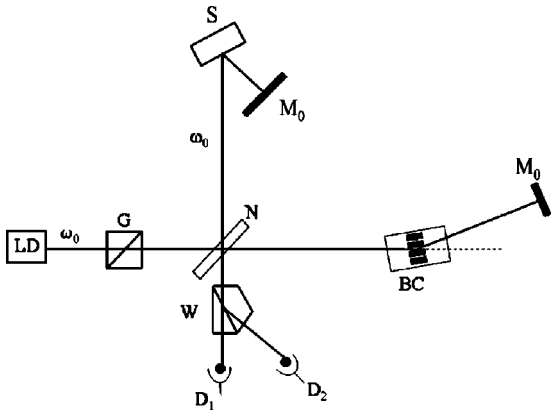

FIG. 1. The setup of the Hazebroek and Holscher interferometric ellipsometer with a Bragg cell. BC: Bragg cell, D: photodiodes, G: Glan–Thomson polarizer, LD: laser diode, M_0: mirror, N: neutral density beam splitter, S: sample, and W: Wollaston prism.

traveled by an acoustic plane wave with a velocity v_s and a wavelength Λ. Because the acoustic angular frequency Ω, given by $\Lambda=2\pi v_s/\Omega$, is typically much smaller than the optical angular frequency ω_0 (by at least five orders of magnitude), a quasi-static approach may be adopted in the light–sound interaction. The phase shift due to the reflection of the light beam from moving surfaces is equal to $\phi(t)=\Omega t$. The associated Doppler-shifted angular frequency for one pass is given by

$$\omega=\omega_0+\frac{d\phi(t)}{dt}=\omega_0+\Omega. \tag{3}$$

Hence the Jones matrix of a Bragg cell is

$$BC=\begin{pmatrix} e^{-i\Omega t} & 0 \\ 0 & e^{-i\Omega t} \end{pmatrix}. \tag{4}$$

2. Theoretical calculations

One possible configuration of an interferometric ellipsometer using a Bragg cell is given by Fig. 1. For the electric field component of the beam on photodiode 1, one finds

$$\mathbf{E}_1=W_t\cdot[N_r\cdot BC\cdot M_0\cdot BC\cdot N_t+N_t\cdot S\cdot M_0\cdot S\cdot N_r]\times G(\pi/4)\cdot\mathbf{E}_L, \tag{5}$$

where

$$\mathbf{E}_L=\begin{pmatrix} 1 \\ 1 \end{pmatrix}\exp(-i\omega_0 t). \tag{6}$$

That leads to

$$E_1=\left[\frac{1}{4}r_s^2\exp(2i\phi_s)+\frac{1}{4}\exp(-2i\Omega t)\right]\exp(-i\omega_0 t)\times\begin{pmatrix} 1 \\ 0 \end{pmatrix}. \tag{7}$$

Similarly one can find for the field propagating towards the photodiode 2

$$\mathbf{E}_2=\left[-\frac{1}{4}r_p^2\exp(2i\phi_p)-\frac{1}{4}\exp(-2i\Omega t)\right]\exp(-i\omega_0 t)\times\begin{pmatrix}0\\1\end{pmatrix}. \quad (8)$$

The time-averaged intensity of these two waves can be obtained by premultiplying their Jones vector $\mathbf{E}$ by their Hermitian adjoint $\mathbf{E}^{\dagger}$, respectively. Then

$$I=cn\,\mathrm{Re}\{\mathbf{E}\cdot\mathbf{E}^{\dagger}\}. \quad (9)$$

In the present case, these intensities consist of a constant contribution plus a term oscillating with the Doppler angular frequency $\delta\omega_0$. The oscillating terms are found to be

$$I_1(\Omega)=\frac{1}{8}cn|r_s|^2\cos(2\Omega t+2\phi_s), \quad (10)$$

$$I_2(\Omega)=\frac{1}{8}cn|r_p|^2\cos(2\Omega t+2\phi_p). \quad (11)$$

The electrical signals are amplified and processed. These ac voltages are given by

$$V_1(\Omega)=K|r_s|^2\cos(2\Omega t+2\phi_s), \quad (12)$$

$$V_2(\Omega)=K|r_p|^2\cos(2\Omega t+2\phi_p). \quad (13)$$

The factor K is a detector-dependent constant and we assume that it is the same for the two photodetectors. The ratio of the amplitudes of $V_2(\Omega)$ and $V_1(\Omega)$ yields $\tan^2(\psi)$ whereas the phase difference $(2\phi_p-2\phi_s)$ equals 2Δ.

3. Subsequent discussion

We show that the Hazebroek and Holscher configuration with a Bragg cell rather than a movable mirror generates valid signals in the two photodiodes from which optical data can be retrieved. The main advantage of this setup compared to the Hazebroek and Holscher configuration is its large bandwidth offering new possibilities for the study of fast surface phenomena. Compared to methods using a Zeeman laser, our method allows one to easily change the wavelength of the laser source while Zeeman lasers exist only for discreet and rare wavelengths. Actually, laser diodes with a wavelength from blue light to far infrared are commercially available.

B. Configuration using a Pockels cell

1. Jones matrix of a Pockels cell

A Pockels cell is often used as a phase-modulator in ellipsometry.[5–8] The Jones matrix of a Pockels cell is

$$P=\begin{pmatrix}e^{-i\phi_o} & 0\\ 0 & e^{-i\Delta\omega_0 t}\end{pmatrix}, \quad (14)$$

where $\Delta\omega_0$ is the modulation depth. It is equal to $m\Omega$ where m is the modulation index and Ω the angular frequency of a periodic saw-tooth voltage signal applied to the crystal.

2. Theoretical calculations

One possible configuration of an interferometric ellipsometer using a Pockels cell is given in Fig. 2. For the electric field component of the beam on photodiodes 1 and 2, one finds

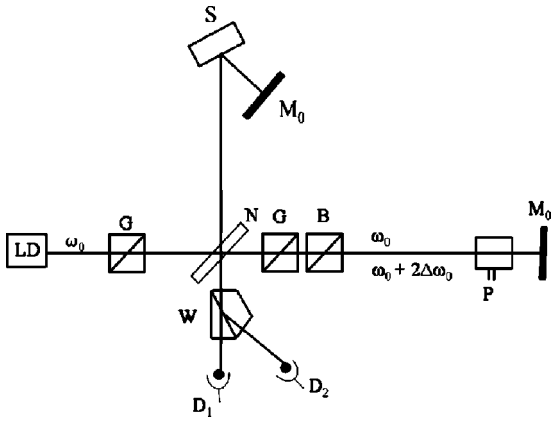

FIG. 2. The setup of the Hazebroek and Holscher interferometric ellipsometer with a Pockels cell. B: polarizing beam splitter, D: photodiodes, G: Glan–Thomson polarizer, LD: laser diode, M_0: mirror, N: neutral density beam splitter, P: Pockels cell, S: sample, and W: Wallaston prism.

$$\mathbf{E}_{1,2}=W_{t,r}\cdot[N_r\cdot G(-\pi/4)\cdot B_p\cdot P\cdot M_0\cdot P\cdot B_p\cdot G(\pi/4)\cdot N_t+N_t\cdot S\cdot M_0\cdot S\cdot N_r]\cdot G(\pi/4)\cdot\mathbf{E}_L, \quad (15)$$

where the index 1, 2 refers, respectively, to t and r. The response of this setup is not different from the previous one. The system generates two signals from which the ellipsometric angles can be obtained directly. This setup keeps all the advantages of the previous one and offers more easiness for an optical adjustment of the components.

IV. A FIBER-OPTIC BASED INTERFEROMETRIC ELLIPSOMETER

One problem with these configurations seems to be finding a line-up that allows on the one hand to vary easily the angle of incidence and on the other hand to make integration easier for *in situ* measurements. We present in this section different configurations in which an optical fiber is added between the neutral beam splitter and the sample. The proposed method allows one to distinguish simultaneously the change of polarization due to the optical fiber to the one due to the sample.

A. Jones matrix of an optical fiber

Optical fiber can be considered as a medium both refracting and absorbing at the same time. Because absorption and refraction properties of the medium are both isotropic, the ellipse of polarization remains unchanged at the output of the optical fiber. This is an ideal case experimentally unverified except under restricting conditions. Actually, mechanical stress or nonuniform temperature variation will induce an anisotropic behavior of the fiber. A more realistic Jones matrix of an optical fiber is given by

$$F=\begin{pmatrix}|r_{fs}|\exp(i\phi_{fs}) & 0\\ 0 & |r_{fp}|\exp(i\phi_{fp})\end{pmatrix}, \quad (16)$$

where $|r_{fs}|\exp(i\phi_{fs})$ and $|r_{fp}|\exp(i\phi_{fp})$ are the transmission coefficients for s and p directions of polarization when a constraint is applied on the optical fiber.

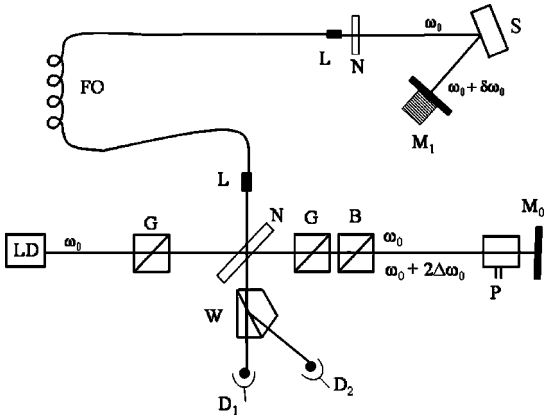

FIG. 3. The setup of the Hazebroek and Holscher interferometric ellipsometer with an optical fiber and a Bragg cell. BC: Bragg cell, D: photodiodes, ED: electromagnetic driver, FO: optical fiber, G: Glan–Thomson polarizer, L: lens, LD: laser diode, M_0: mirror, N: neutral density beam splitter, S: sample, and W: Wollaston prism.

B. Practical considerations

Consider the configuration composed of a Bragg cell and where an optical fiber is added between the neutral density beam splitter and the sample. The formal response of the entire configuration becomes

$$\mathbf{E}_{1,2}=W_{t,r}\cdot[N_r\cdot BC\cdot M_0\cdot BC\cdot N_t+N_t\cdot F\cdot S\cdot M_0\cdot S\cdot F\cdot N_r]\cdot G(\pi/4)\cdot\mathbf{E}_L. \tag{17}$$

That leads to

$$I_1(\Omega)=\frac{1}{8}cn|r_s|^2|r_{fs}|^2\cos(2\Omega t+2\phi_s-2\phi_{fs}), \tag{18}$$

$$I_2(\Omega)=\frac{1}{8}cn|r_p|^2|r_{fp}|^2\cos(2\Omega t+2\phi_p-2\phi_{fp}). \tag{19}$$

It becomes impossible to distinguish the change of polarization due to the sample to the one due to the optical fiber.

C. The Hazebroek and Holscher ellipsometer with an optical fiber

One solution to distinguish each change of polarization consists of using a second modulation during the path of the light between the end of the optical fiber and the mirror. This can be achieved using, for example, the Hazebroek and Holscher method as shown in Fig. 3. A 50/50 neutral beam splitter in normal incidence reflects half the beam intensity and transmits the other one. As the polarization remains unchanged between the input and output of the lenses, we do not include them into the calculation. The formal expression for the electric field amplitudes is then

$$\mathbf{E}_{1,2}=W_{t,r}\cdot[N_r\cdot BC\cdot M_0\cdot BC\cdot N_t+N_t\cdot F\cdot(N_t\cdot S\cdot M_{\mathrm{mod}}\cdot S\cdot N_t+M_0\cdot N_r)\cdot F\cdot N_r]\cdot G(\pi/4)\cdot\mathbf{E}_L, \tag{20}$$

where $M_{\mathrm{mod}}=M_0\exp(-i\delta\omega_0 t)$. This leads to the following intensities in the detectors:

$$I_1(\Omega,\delta\omega_0)=cn[\tfrac{1}{32}|r_s|^2|r_{fs}|^2\cos(2\Omega t-\delta\omega_0 t+2\phi_s-2\phi_{fs})+\tfrac{1}{16}|r_{fs}|^2\cos(2\Omega t-2\phi_{fs})+\tfrac{1}{64}|r_s|^2|r_{fs}|^4\cos(\delta\omega_0 t-2\phi_s)], \tag{21}$$

$$I_2(\Omega,\delta\omega_0)=cn[\tfrac{1}{32}|r_p|^2|r_{fp}|^2\cos(2\Omega t-\delta\omega_0 t+2\phi_p-2\phi_{fp})+\tfrac{1}{16}|r_{fp}|^2\cos(2\Omega t-2\phi_{fp})+\tfrac{1}{64}|r_p|^2|r_{fp}|^4\cos(\delta\omega_0 t-2\phi_p)]. \tag{22}$$

The electrical signals are amplified and filtering at, respectively, three angular frequencies: $\omega_\alpha=2\Omega$, $\omega_\beta=\delta\omega_0$, and $\omega_\gamma=2\Omega-\delta\omega_0$ leads to three signals for each photodiode

$$V_{1,\alpha}(\omega_\alpha)=K|r_{fs}|^2\cos(\omega_\alpha t-2\phi_{fs}), \tag{23}$$

$$V_{1,\beta}(\omega_\beta)=K|r_s|^2|r_{fs}|^4\cos(\omega_\beta t-2\phi_s), \tag{24}$$

$$V_{1,\gamma}(\omega_\gamma)=K|r_s|^2|r_{fs}|^2\cos(\omega_\gamma t+2\phi_s-2\phi_{fs}) \tag{25}$$

for photodiode 1 and

$$V_{2,\alpha}(\omega_\alpha)=K|r_{fp}|^2\cos(\omega_\alpha t-2\phi_{fp}), \tag{26}$$

$$V_{2,\beta}(\omega_\beta)=K|r_p|^2|r_{fp}|^4\cos(\omega_\beta t-2\phi_p), \tag{27}$$

$$V_{2,\gamma}(\omega_\gamma)=K|r_p|^2|r_{fp}|^2\cos(\omega_\gamma t+2\phi_p-2\phi_{fp}) \tag{28}$$

for photodiode 2.

The ratio of the amplitudes of $V_{1,\alpha}$ and $V_{2,\alpha}$ yields $\tan^2(\psi_f)$ and the phase difference $(2\phi_{fp}-2\phi_{fs})$ equals $2\Delta_f$. Similarly, the ratio of the amplitudes of $V_{1,\beta}/V_{2,\beta}$ and $V_{1,\gamma}/V_{2,\gamma}$ yields $\tan^2(\psi)\times\tan^4(\psi_f)$ and $\tan^2(\psi)\times\tan^2(\psi_f)$, respectively. The ellipsometric angle Δ of the sample can be determined even using the phase difference of $V_{1,\beta}$ and $V_{2,\beta}$ yielding to 2Δ even using the phase difference between $V_{2,\gamma}$ and $V_{1,\gamma}$ yielding to $2(\Delta-\Delta_f)$.

D. Subsequent discussion

This configuration is capable of generating valid signals in the two photodiodes from which the ellipsometric angles of the sample can be retrieved. A major disadvantage of this system is its weak bandwidth due to the mechanical modulation of the mirror, as seen previously in the primary Hazebroek and Holscher configuration. Another disadvantage is that it has an active component between the end of the optical fiber and the sample making it more difficult to integrate for *in situ* measurements.

V. *IN SITU* AND REAL-TIME HETERODYNE ELLIPSOMETER

A. Practical considerations

The last configurations proposed here do not contain any active element between the end of the optical fiber, the sample, and the last mirror. They are based on the use of two laser diodes with two wavelengths slightly different.

B. Configuration using a Bragg cell

A chromatic beam splitter, a semitransparent selective optical filter, is put at the output of the fiber and before the sample (Fig. 4). It reflects the field component at ω_1 and

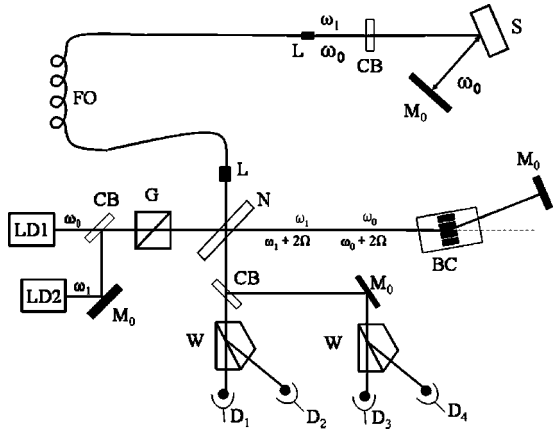

FIG. 4. *In situ* and real-time heterodyne ellipsometer using a Bragg cell. BC: Bragg cell, CB: chromatic beam splitter, D: photodiodes, FO: optical fiber, G: Glan–Thomson polarizer, L: lens, LD: laser diode, M_0: mirror, N: neutral density beam splitter, S: sample, and W: Wollaston prism.

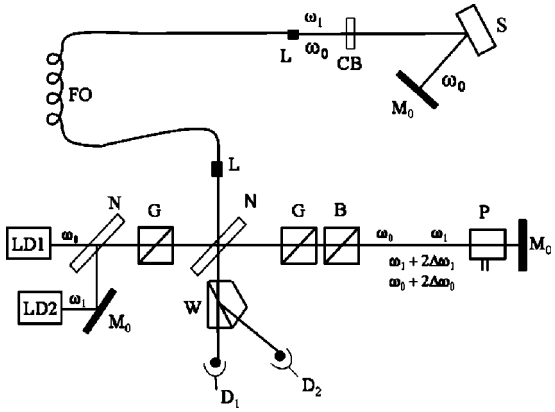

FIG. 5. *In situ* and real-time heterodyne ellipsometer using a Pockels cell. B: polarizing beam splitter, CB: chromatic beam splitter, D: photodiodes, FO: optical fiber, G: Glan–Thomson polarizer, L: lens, LD: laser diode, M_0: mirror, N: neutral density beam splitter, P: Pockels cell, S: sample, and W: Wollaston prism.

totally transmits the one at ω_0. The Jones matrix for this optical component can be viewed as a perfect mirror at normal incidence for the reflected beam and as an isotropic plate with null extinction coefficient for the transmitted beam.

For the electric field component of the beam on photodiode 1 and photodiode 2, one finds

$$\mathbf{E}_{1,2}=W_{t,r}\cdot[N_r\cdot BC\cdot M_0\cdot BC\cdot N_t+N_t\cdot F\cdot S\cdot M_0\cdot S\cdot F\cdot N_r]\cdot G(\pi/4)\cdot E_{L0}, \tag{29}$$

where

$$\mathbf{E}_{L0}=\begin{pmatrix}1\\1\end{pmatrix}\exp(-i\omega_0 t). \tag{30}$$

Similarly, for the electric field component of the beam on photodiode 3 and photodiode 4, one finds

$$\mathbf{E}_{3,4}=W_{t,r}\cdot M_0\cdot M_0\cdot[N_r\cdot BC\cdot M_0\cdot BC\cdot N_t+N_t\cdot F\cdot M_0\cdot F\cdot N_r]\cdot G(\pi/4)\cdot M_0\cdot\mathbf{E}_{L1}, \tag{31}$$

where

$$\mathbf{E}_{L1}=\begin{pmatrix}1\\1\end{pmatrix}\exp(-i\omega_1 t). \tag{32}$$

That leads to the signals for photodiodes 1 and 2,

$$V_1(\Omega)=K|r_{fs}|^2|r_s|^2\cos(2\Omega t-2\phi_{fs}+2\phi_s), \tag{33}$$

$$V_2(\Omega)=K|r_{fp}|^2|r_p|^2\cos(2\Omega t-2\phi_{fp}+2\phi_p), \tag{34}$$

and for photodiodes 3 and 4,

$$V_3(\Omega)=K|r_{fs}|^2\cos(2\Omega t-2\phi_{fs}), \tag{35}$$

$$V_4(\Omega)=K|r_{fp}|^2\cos(2\Omega t-2\phi_{fp}). \tag{36}$$

The ratio of the amplitudes of $V_2\times V_3/V_1\times V_4$ yields $\tan^2(\psi)$, whereas the phase difference $\arg(V_2-V_1)-\arg(V_4-V_3)$ equals $2\Delta=2(\phi_p-\phi_s)$.

C. Configuration using a Pockels cell

As the two wavelengths are slightly different, the Pockels cell will generate a modulation depth different for each wavelength. For example, a Pockels cell composed by $LibNO_3$ crystal of length $l=1$ cm and height $d=3$ mm, mounted in a transverse configuration and illuminated by two waves at, respectively, $\lambda_0=650$ nm and $\lambda_1=680$ nm gives $\Delta\omega_0=264$ kHz and $\Delta\omega_1=253$ kHz (taking $r_{33}=30.9\times10^{-12}$ m V^{-1}, $n_e=2.2$, $V_0=500$ V, and $\Omega=50$ kHz). For the electric field component of the beam on photodiode 1 and photodiode 2 (Fig. 5), one finds

$$\begin{aligned}\mathbf{E}_{1,2}=W_{t,r}\cdot[&N_r\cdot G(-\pi/4)\cdot B_p\cdot P_0\cdot M_0\cdot P_0\cdot B_p\\&\times G(\pi/4)\cdot N_t+N_t\cdot F\cdot S\cdot M_0\cdot S\cdot F\cdot N_r]\\&\times G(\pi/4)\cdot E_{L0}+[N_r\cdot G(-\pi/4)\cdot B_p\cdot P_1\cdot M_0\cdot P_1\\&\times B_p\cdot G(\pi/4)\cdot N_t+N_t\cdot F\cdot M_0\cdot F\cdot N_r]\\&\times G(\pi/4)\cdot M_0\cdot\mathbf{E}_{L1},\end{aligned} \tag{37}$$

where P_0, P_1 are the Jones matrices of the Pockels cell associated to each laser. Full expression of the intensities shows terms oscillating at cross frequencies $(\omega_1\pm\omega_0,\omega_1+2\Delta\omega_1-\omega_0,\ldots)$. If the bandwidth of the photodiodes is below 1 GHz, the resulting intensities are found to be

$$\begin{aligned}I_1(\Delta\omega_0,\Delta\omega_1)=cn[&\tfrac{1}{32}|r_{fs}|^2\cos(2\Delta\omega_1 t-2\phi_{fs})\\&+\tfrac{1}{32}|r_{fs}|^2|r_s|^2\cos(2\Delta\omega_0 t-2\phi_{fs}\\&+2\phi_s)],\end{aligned} \tag{38}$$

$$\begin{aligned}I_2(\Delta\omega_0,\Delta\omega_1)=cn[&\tfrac{1}{32}|r_{fp}|^2\cos(2\Delta\omega_1 t-2\phi_{fp})\\&+\tfrac{1}{32}|r_{fp}|^2|r_p|^2\cos(2\Delta\omega_0 t-2\phi_{fp}\\&+2\phi_p)].\end{aligned} \tag{39}$$

The electrical signals are amplified and filtering at, respectively, two angular frequencies: $\omega_\alpha=2\Delta\omega_0$ and $\omega_\beta=2\Delta\omega_1$ leading to two signals for each photodiode,

$$V_{1,\alpha}(\omega_\alpha)=K|r_{fs}|^2|r_s|^2\cos(\omega_\alpha t-2\phi_{fs}+2\phi_s), \tag{40}$$

$$V_{1,\beta}(\omega_\beta)=K|r_{fs}|^2\cos(\omega_\beta t-2\phi_{fs}) \tag{41}$$

for photodiode 1 and

$$V_{2,\alpha}(\omega_\alpha)=K|r_{fp}|^2|r_p|^2\cos(\omega_\alpha t-2\phi_{fp}+2\phi_p), \tag{42}$$

$$V_{2,\beta}(\omega_\beta) = K|r_{fp}|^2 \cos(\omega_\beta t - 2\phi_{fp}) \tag{43}$$

for photodiode 2.

The ratio of the amplitudes of $V_{1,\beta}$ and $V_{2,\beta}$ yields $\tan^2(\psi_f)$ whereas the phase difference $(2\phi_{fp} - 2\phi_{fs})$ equals $2\Delta_f$. Similarly, the ratio of the amplitudes of $V_{1,\alpha}/V_{2,\alpha}$ yields $\tan^2(\psi) \times \tan^2(\psi_f)$. The ellipsometric angle Δ of the sample can be determined using the phase difference between $V_{2,\alpha}$ and $V_{1,\alpha}$ yielding to $2(\Delta - \Delta_f)$.

[1] H. Hazebroek and A. Holscher, J. Phys. E **6**, 822 (1973).
[2] R. Azzam and N. Bashara, *Ellipsometry and Polarized Light* (Elsevier, Amsterdam, 1989).
[3] M. Wind and K. Hemmes, Meas. Sci. Technol. **5**, 37 (1994).
[4] N. Umeda and H. Takasaki, Surf. Sci. **96**, 141 (1980).
[5] H. Mathieu, D. McClure, and R. Muller, Rev. Sci. Instrum. **45**, 798 (1974).
[6] A. Moritani, Y. Okuda, and J. Nakai, Appl. Opt. **22**, 1329 (1983).
[7] E. Compain and B. Drevillon, Rev. Sci. Instrum. **38**, 2410 (1998).
[8] J. R. Mackey, K. K. Das, S. A. Anna, and G. H. McKinley, Meas. Sci. Technol. **10**, 946 (1999).